Limnol. Oceanogr., 34(1), 1989, 68–81

Marine humic and fulvic acids: Their effects on remote sensing of ocean chlorophyll

Kendall L. Carder and Robert G. Steward
University of South Florida, Marine Science Department,
140 Seventh Avenue South, St. Petersburg 33701

George R. Harvey and Peter B. Ortner
National Oceanic and Atmospheric Administration,
Atlantic Oceanographic and Meterological Laboratories,
4301 Rickenbacker Causeway, Miami, Florida 33249

Abstract

Marine humic and fulvic acids were concentrated from about 1,400 liters of seawater from the Gulf of Mexico, and specific absorption coefficients were measured for each from 240 to 675 nm. Spectral absorption coefficients were then calculated for Gulf of Mexico stations where earlier data on humic and fulvic acid concentrations were available. Marine humic and fulvic acid values have low molecular weights consistent with extrapolations from soil-derived curves of their specific absorption coefficients vs. molecular weight. Marine fulvic and humic acids appear to account for most if not all water color or Gelbstoff in the offshore regions of the Gulf of Mexico. Based on a remote-sensing reflectance model, it appears that the increase in the Gelbstoff: chlorophyll ratio for waters adjacent to and downstream from regions of high primary productivity accounts for much of the deviation found for such waters from the global chlorophyll algorithm of the Coastal Zone Color Scanner.

The effect of "yellow substance" also known as aquatic humus or Gelbstoff (composed chiefly of fulvic and humic acids) on water color has been documented, especially for inland waters where the high concentrations are easy to measure (*see* Zepp and Schlotzhauer 1981; Kirk 1980 and references therein). For the oceans, the highest concentrations of yellow substance occur in regions influenced by land drainage, such as the Baltic Sea and certain coastal waters (e.g. James and Birge 1938; Jerlov 1955; Kalle 1966; Hojerslev 1974; Stuermer 1975; Lundgren 1976). For oceanic waters unaffected by significant land drainage, there are few direct measurements of the optical influence of yellow substance at visible wavelengths. In highly productive upwelling areas, Bricaud et al. (1981) have measured the absorption throughout the ultraviolet and visible spectrum, but in regions of lower productivity they have extrapolated measurements from the more absorptive ultraviolet wavelengths into the visible spectrum. Other values for clear oceanic waters have either been measured at short wavelengths (*see* Jerlov 1968, table 13) or have been indirectly calculated (e.g. Morel and Prieur 1975; Smith and Baker 1982; Carder et al. 1986*b*).

As a result of the apparently low values for absorption due to yellow substance, the assumption has often been made (Smith and Baker 1982; Bricaud et al. 1981) that water color or Gelbstoff in the oligotrophic ocean covaries linearly with chlorophyll pigments or its absorption is negligible at 440 nm—a wavelength region of prime importance for the remote sensing of ocean chlorophyll. This region is near the absorption maximum of the Chl *a* Soret band and represents the shortest wavelength channel on the Nimbus-7 Coastal Zone Color Scanner (CZCS) used to measure chlorophyll from space. Since Gelbstoff absorption at 440 nm as small as 0.005 m^{-1} is equivalent to the absorption coefficient due to phytoplankton when Chl $a \doteq 0.10$ mg m^{-3}, it is important to understand the role of marine humus as it affects the remote sensing of ocean color, even at "negligible" concentrations. Accurate measurement of Gelbstoff absorption

Acknowledgment

Financial support for this research was provided by grant NAGW-465 from NASA to the University of South Florida.

coefficients $\lesssim 0.01\ m^{-1}$ is, however, very difficult.

An alternative approach to direct measurement of the absorption coefficient due to yellow substance or humus in oligotrophic waters is to extract and concentrate fulvic and humic acids and independently determine their specific absorption coefficients. Although fulvic and humic acids may not be the only absorbing dissolved organic constituents, their absorption coefficients provide a measure of the minimal absorption levels expected from natural dissolved organic substances. The spectral shapes and intensities of the individual absorption curves also provide an indication of the molecular weights of the humic or fulvic materials (Hayase and Tsubota 1985) and, consequently, may be useful in deducing the presence of terrigenous aquatic humus in the marine environment.

In oceanic areas unaffected by freshwater runoff the concentration of yellow substance is presumably related to primary productivity as a by-product of algal cell degradation (Fogg and Boalch 1958; Yentsch and Reichert 1962; Harvey et al. 1983 and references therein). Bricaud et al. (1981) have shown for certain upwelling areas, however, that for chlorophyll concentration changes of two orders of magnitude, there may be little change in concentrations of yellow substance. This finding suggests a long period for accrual and perhaps a long half-life for humus in the ocean relative to the algal population that produced it. Such a scenario may result in patches of marine humus indicative of past primary productivity that is not manifest in the present chlorophyll content of the patch.

With the chlorophyll remote-sensing algorithms based on spectral ratios (*see* Gordon and Morel 1983), the absorption effects of Gelbstoff cannot be separated from those of chlorophyll. Thus overestimates or underestimates of the chlorophyll in the patch will result if the marine humus does not covary linearly with the concentration of chlorophyll pigment. Covariance of marine humus and other ocean color constituents with Chl *a*-like pigments (Chl *a* + pheophytin *a*) is a condition that must be fulfilled for waters to be classified as Morel Case 1 waters (*see* Morel 1980) and for the global chlorophyll algorithm to be applied to data that are remotely sensed. Otherwise, site- and season-specific algorithms must be used.

We have measured the specific absorption curves as a function of wavelength for concentrated marine humic acid (MHA) and marine fulvic acid (MFA) and compared them to reported values of terrigenous humic and fulvic acids. The absorption coefficient values due to humic and fulvic acids are calculated for various locations in the Gulf of Mexico where marine humus has been extracted and concentrations measured (*see* Harvey et al. 1983). These values are compared to published values of absorption due to Gelbstoff to substantiate that MHA and MFA can account for most of this absorption. The effects of marine humus on the accuracy of remote-sensing algorithms for chlorophyll are evaluated as is the relationship between concentrations of marine humus and the recent history of primary productivity for a water parcel.

Methods

Samples of MHA and MFA from loop current and Mississippi River plume sites were each concentrated from about 1,400 liters of seawater from the surface layer (<50 m) and isolated with the methods discussed by Harvey et al. (1983). Samples were collected with a stainless steel, gas-lift (N_2) pumping system that avoided the oxidative effects of contact with natural light and atmosphere. The samples were acidified to pH 2 and extracted through Amberlite XAD-2 resin columns. To remove salts, we rinsed the columns with 2 liters of 0.01 N HCl. The MFA and MHA collected were eluted with 2.4 liters of 1 N NH_4OH in methanol after an initial 4-h soak in methanol. Elution with another 2 liters of methanol assured complete recovery (Harvey et al. 1983).

Eluents were combined and dried at temperatures <40°C in a rotary evaporator. MFA and MHA were redissolved in deionized water containing a few microliters of NaOH and then acidified to pH 2 with 1.0 N HCl. The solution was then refrigerated for 48 h to allow complete precipitation of MHA. Centrifugation and decantation were

Symbols used in this paper.

	Definition	Units
λ	Wavelength of light	nm
A	Empirical, multiplicative constant for relationship between chlorophyll-like pigments and spectral upwelling radiance ratios (*see Eq. 5*)	mg m^{-3}
$a_g(\lambda)$, $a_\phi(\lambda)$	Absorption coefficient for Gelbstoff or phytoplankton at wavelength λ	m^{-1}
a^*_f, a^*_h	Mass-specific absorpton coefficients for MFA or MHA at 450 nm	m^2 g^{-1}
$a^*_p(\lambda)$	Chlorophyll pigment-specific absorption coefficient of particles at λ	m^2 (mg Chl *a*)$^{-1}$
$a^*_\phi(\lambda)$	Chlorophyll pigment-specific absorption coefficient of phytoplankton at λ	m^2 (mg Chl *a*)$^{-1}$
$a_w(\lambda)$	Absorption coefficient for seawater at λ	m^{-1}
B	Empirical exponent for the [Chl *a*] vs. r_{ij} relation (*see Eq. 5*)	
$b'_p(\lambda)$, $b'_w(\lambda)$	Backscattering coefficient of particles or seawater at λ	m^{-1}
C_f, C_h, C_g	Concentration of MFA, MHA, or Gelbstoff	g m^{-3}
[Chl *a*]	Concentration of chlorophyll *a* and pheophytin *a*	mg m^{-3}
$E_T(\lambda)$	Total downwelling irradiance	W m^{-2} nm^{-1}
f	Fulvic acid fraction of marine humus	
I	Coefficient for converting subsurface upwelling irradiance to water-leaving radiance	st^{-1}
$k1$, $k2$	$S_f(450 - \lambda)$, $S_h(450 - \lambda)$	
$L_u(\lambda)$	Subsurface upwelling radiance at λ	W m^{-2} st^{-1} nm^{-1}
$L_w(\lambda)$	Water-leaving (upwelling) radiance at λ just above the sea surface	W m^{-2} st^{-1} nm^{-1}
r_{ij}	Ratio of subsurface upwelling radiance at wavelengths λ_i and λ_j	
$R_{RS}(\lambda)$	Remote-sensing reflectance at λ	
S	Spectral slope of an exponential expression for the wavelength dependence of the Gelbstoff absorption coefficient	nm^{-1}
S_f, S_g, S_h	Spectral slopes for MFA, Gelbstoff, or MHA	nm^{-1}

used to separate the MHA precipitate from the soluble MFA, and both fractions were washed with CH_2Cl_2, freeze-dried, and weighed. The samples were stored at −20°C, and care was taken to avoid light and air throughout the isolation.

To measure the optical properties of MHA and MFA, we weighed and redissolved the samples in double-distilled, deionized water adjusted to a measured pH of 9.0 with 1% NaOH. A drop in pH resulting from the combined effects of the dissociation products of humic/fulvic acids and a small residual quantity of HCl bound to amino acid complexes yields a pH value of about 8.3 for the final solution. The test solutions ranged in concentration from 38 to 44 mg liter^{-1} with an ionic strength estimated at about 5×10^{-5}. Absorbances of each of the solutions from 750 to 250 nm were measured with 10-cm path-length cells in a Cary spectrophotometer (model 17D) with a deionized water blank. Each sample was scanned twice consecutively and averaged. The water blank was treated identically.

The effects of pH on specific absorption for humic acid are very small (in the range 6–11), but values for fulvic acid at pH 11 are as much as 50% higher than are those at pH 6 (Zepp and Schlotzhauer 1981). Errors due to pH for our specific absorption values for fulvic acid are estimated to be <5% relative to values expected for the acids in seawater. Scattering effects due to undissolved particles are thought to be negligible as the initial grains were few and large and seemed to dissolve entirely. The resultant solution was yellow and had no particles visible to the naked eye. Only particles smaller than the wavelength of light have a significant spectral effect on scattering and must be large in number to impact absorbance values in the range measured. Further evidence of negligible scattering effects is that replicate samples were quite consistent.

The effects of separating MFA and MHA and then reconstituting them as outlined is not expected to change the optical properties of the optically resonant ring structures (W. Sackett pers. comm.). Again, because the ring structure should be unaffected by

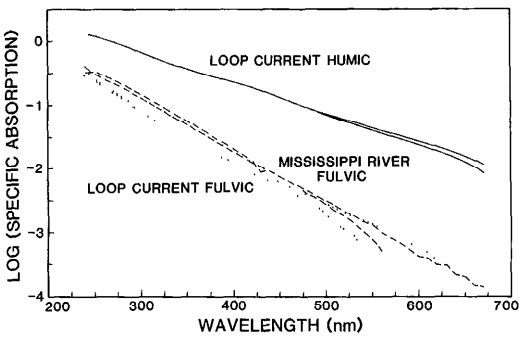

Fig. 1. Specific absorption curves vs. wavelength for marine humic acid and marine fulvic acid.

ionic strength, these results should also be applicable to seawater.

Absorbance values were normalized to the same concentration of dissolved humic or fulvic matter (mg liter^{-1} or g m^{-3}) and then converted to mass-specific absorption coefficients (liters mg^{-1} m^{-1} or m^2 g^{-1}). If normalized to dissolved organic carbon concentration, the specific absorption coefficients would be about twice those normalized to mass concentration of dissolved humus. Finally, the mass-specific absorption curves as a function of wavelength were fitted by an exponential curve of the form

$$a^*(\lambda) = a^*_{450}\exp[S(450 - \lambda)]$$

(Zepp and Schlotzhauer 1981; Hayase and Tsubota 1985; Bricaud et al. 1981). (List of symbols gives definitions and units.)

Multiplication of measured marine humic C_h or fulvic acid C_f concentration (g m^{-3}) by the appropriate specific absorption curve provides values of the spectral absorption coefficient for wavelengths between about 300 and 700 nm at natural concentrations. To obtain the absorption coefficient of marine humus or Gelbstoff, we summed the humic and fulvic absorption contributions.

Results and discussion

The exponential spectral slope coefficients S (nm^{-1}) for the fulvic acid curves were nearly twice as large as those for humic acid (Fig. 1, Table 1). The specific absorption parameter a^*_h (specific absorption at 450 nm) for humic acid, however, was 24 times as large as the fulvic acid a^*_f parameter for the loop current. It was about 18 times the a^*_f value for the Mississippi plume sample.

The absorption curves for MHA and MFA can be compared to similar curves for aquatic and sediment-derived humus. The data of Hayase and Tsubota (1985) suggest a dependence of a^*_h and a^*_f on the molecular weight of sediment-derived humus—a dependence borne out in our data (Fig. 2). Note that our values are normalized per unit of dissolved organic carbon rather than per unit of dissolved organic matter so that our data can be directly compared to their sediment-derived humus values.

The low molecular weight of marine humus clearly provides points that appear as curve extensions from the higher molecular weight samples of sediment-derived humus. The specific absorption coefficient of humic acid varies inversely with molecular weight, while that of fulvic acid is directly proportional to molecular weight. The spectral slope parameter S_f for fulvic acid decreases slightly with increasing molecular weight. On the basis of the spectral slope of the data of Hayase and Tsubota (1985) between 320 and 480 nm, S_h does not change significantly with molecular weight for samples of sediment-derived humic acid. Their values were only about 0.008 nm^{-1}, however, while ours were 0.0110 nm^{-1}, the same as humic slope values reported by Zepp and Schlotzhauer (1981) for a wide variety of aquatic, soil-derived, and marine humic

Table 1. Parameters for the equation $a^*_{450} = \exp[S(450 - \lambda)]$ for fulvic acid from two stations and humic acid from one station in the Gulf of Mexico. Mean and range values of two replications are shown with the mean correlation coefficient, r^2.

Station	Type	a^*_{450} (m^2 g^{-1})	S (nm^{-1})	r^2
Mississippi plume	Fulvic	0.007±0.001	0.0194±0.00044	0.999
Gulf loop intrusion	Fulvic	0.005±0.001	0.0184±0.00166	0.997
	Humic	0.1302±0.00005	0.0110±0.00012	0.999

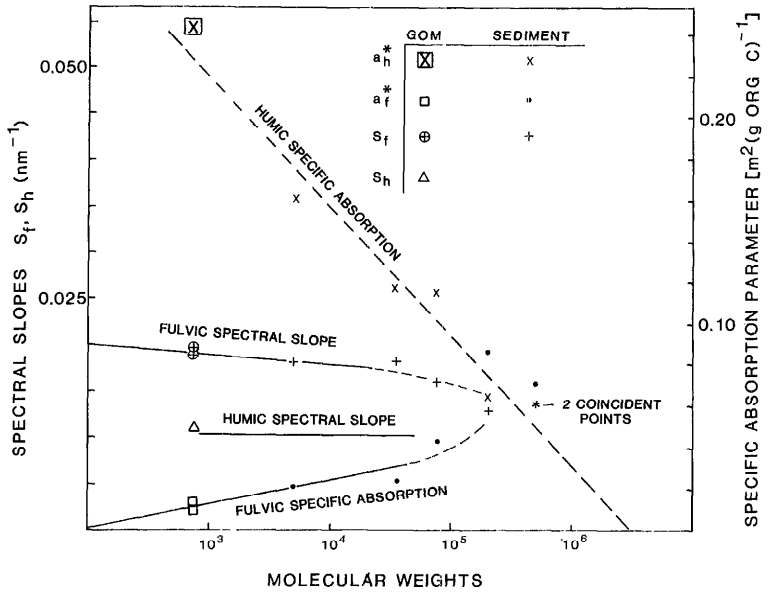

Fig. 2. Variation of the specific absorption and the spectral slope parameters as a function of molecular weight. The lines shown are visual estimates of the trends of low molecular weight data. Dashed line extensions are visual estimates of the nonlinear nature of the data at high molecular weights. The S_h curve at 0.010 nm^{-1} represents the average of humic acid standard samples of varied (unknown) molecular weights based on the data of Zepp and Schlotzhauer (1981) (range, 0.009–0.012 nm^{-1}).

samples. No molecular weights were reported by Zepp and Schlotzhauer; the weights are expected to fall, however, within the range reported by Hayase and Tsubota (1985). The direct variability of a^*_f and inverse variability of a^*_h with molecular weight may be useful in identifying samples containing soil-derived, terrigenous humus, which have much higher molecular weights than MHA and MFA from the euphotic zone.

For marine samples not influenced by runoff from land, the spectral slope of the absorption curve of marine Gelbstoff will provide a measure of the relative fractions of MHA and MFA in the sample. This curve can be expressed as

$$a_g(\lambda) = C_f a^*_f \exp(k1) + C_h a^*_h \exp(k2) \quad (1)$$

where $k1 = S_f(450 - \lambda)$ and $k2 = s_h(450 - \lambda)$. C_f and C_h are the MHA and MFA concentrations (g m^{-3}). For $a^*_f = 0.00728$ m^2 g^{-1}, $a^*_h = 0.1304$ m^2 g^{-1}, $S_f = 0.01890$ nm^{-1}, and $S_h = 0.01105$ nm^{-1}, a family of curves for $a_g(\lambda)$ can be generated as a function of f, the fulvic acid fraction $[C_f/(C_f + C_h)]$ of the total Gelbstoff. These curves are shown for $C_f + C_h = 1$ g m^{-3} in Fig. 3. Note the relative insensitivity of $a_g(\lambda)$ to fulvic acid and the slight semilogarithmic curvature for the middle curves. This curvature indicates that at shorter wavelengths fulvic acid plays a more significant absorption role relative to that of humic acid than it does at longer wavelengths because $S_f \doteq 1.5\ S_h$. It appears from Fig. 3 that humic acid is the dominant contributor to $a_g(\lambda)$, but a brief glance at Table 2 shows that this appearance is erroneous. Under most circumstances fulvic acid makes up a very large fraction of marine humus, compensating for its relatively small a^*_f value.

The slight curvature of the lines in Fig. 3 results in spectral slope values, S_g, for an exponential curve fit to $a_g(\lambda)$ data that are dependent on the spectral portion of the curve being fit.

$$S_g(f, \lambda_1, \lambda_2) \doteq \ln \frac{a_g(f, \lambda_1)}{a_g(f, \lambda_2)} \cdot (\lambda_2 - \lambda_1)^{-1}$$

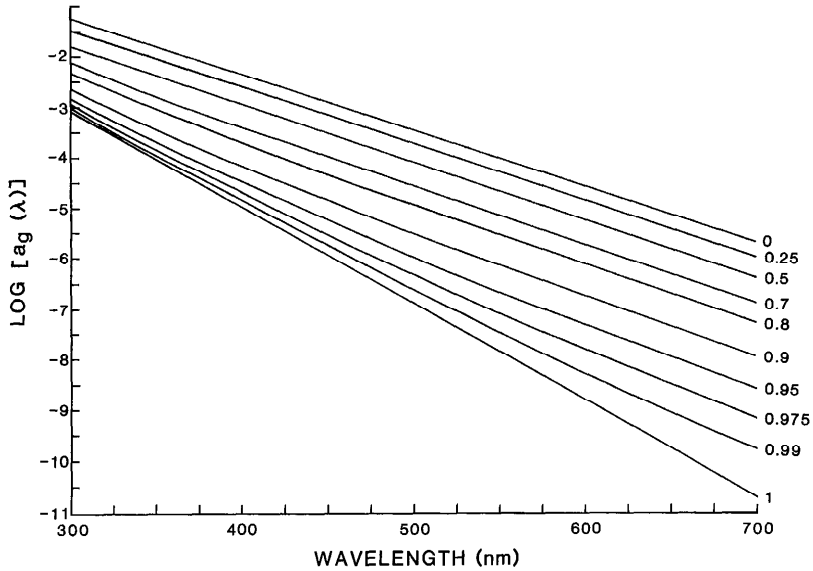

Fig. 3. Spectral variation of the absorption coefficient due to marine humus or Gelbstoff as a function of the fulvic acid fraction of Gelbstoff for $a^*_f = 0.00732$ m^2 g^{-1}, $a^*_h = 0.131$ m^2 g^{-1}, $B_f = 0.0186$ nm^{-1}, and $B_h = 0.0110$ nm^{-1}. The fulvic acid fraction is shown beside each curve.

is dependent both on the fulvic acid fraction f of the marine humus and on the spectral range of interest. It is clear (Fig. 4) that estimating S_g with $a_g(370)$ and $a_g(440)$ values provides a slightly different slope than estimating S_g with $a_g(440)$ and $a_g(565)$ values, except for f values of 1.0 and 0. Under these extremes Eq. 1 reduces to a simple exponential curve.

Calculating S_g (Table 3) from the semilogarithmic slope between $a_g(370)$ and $a_g(440)$ provides slope values for the region of the spectrum used in spectral extrapolations from $a_g(375)$ reported by Bricaud et al. (1981). They used a mean S_g value of 0.014 nm^{-1}, practically identical to the mean slope 0.0141 nm^{-1} for the Gulf of Mexico (GOM) samples. The GOM slope values varied from 0.0115 to 0.0173 nm^{-1} for the 370–440-nm spectral region, depending on the fulvic acid fraction (*see Table 3*). Bricaud et al. (1981) reported slope values ranging from 0.0180

Table 2. Values of the absorption coefficients for concentrations of fulvic and humic acids in the Gulf of Mexico.

Station	Depth (m)	Chl *a**	Humic*	Fulvic*	$a_h(440)$	$a_f(440)$	$a_g(440)$	$a_h(565)$	$a_f(565)$	$a_g(565)$
			(g m^{-3})				(m^{-1})			
Mississippi	3	1.35	0.114	0.550	0.0165	0.00484	0.0218	0.00445	0.000475	0.00492
plume	3	1.20	0.126	1.270	0.0183	0.01118	0.0295	0.00491	0.001096	0.00610
($S > 24‰$)	4	7.90	0.176	0.904	0.0255	0.00796	0.0335	0.00685	0.000780	0.00764
Gulf loop	20	0.24	0.026	0.724	0.0038	0.00654	0.0103	0.00101	0.000640	0.00165
intrusion	20	0.21	0.003	0.190	0.0004	0.00168	0.0021	0.00012	0.000164	0.00028
	20	0.08	0.014	0.234	0.0020	0.00206	0.0041	0.00054	0.000202	0.00075
	55	0.08	0.009	0.058	0.0013	0.00051	0.0019	0.00035	0.000050	0.00040
Yucatan	10	0.06	0.029	0.223	0.0042	0.00196	0.0062	0.00113	0.000192	0.00132
Campeche	5	0.20	0.105	0.754	0.0152	0.00664	0.0219	0.00410	0.000651	0.00475
Cape San	4	0.40	0.336	0.577	0.0487	0.00490	0.0537	0.01311	0.000481	0.01358
Blas	55	1.06	0.010	0.139	0.0014	0.00122	0.0027	0.00038	0.000120	0.00051

* Data for marine humic and fulvic acids from Harvey et al. 1983.

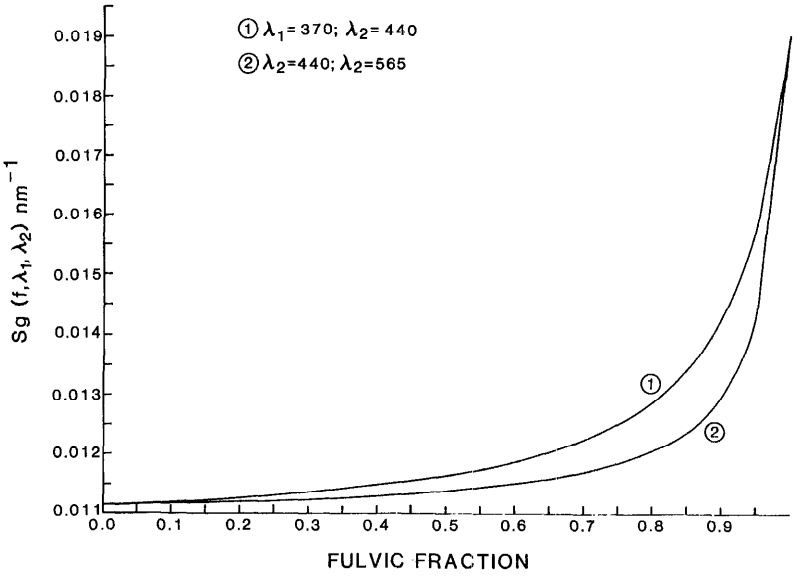

Fig. 4. Variation of the spectral slope parameter for marine Gelbstoff as a function of the fulvic acid fraction.

nm^{-1} in the Baltic Sea to 0.012 ± 0.0023 nm^{-1} in the southern Indian Ocean. Thus, the range of GOM slope values is representative of the range found elsewhere. Although the reported Baltic values are quite high and may reflect significant terrigenous inputs of Gelbstoff, they do suggest a very large fulvic acid fraction. On the other hand, the southern Indian Ocean values suggest a low fulvic acid fraction in dissolved humus.

If slope values are calculated for the spectral region used in the remote sensing of ocean color, 440–565 nm, slightly lower values of S_g are encountered (Table 3), with a mean GOM value of 0.0129 nm^{-1}. The lower slope values in this spectral range reflect the relatively larger effect of humic acid on absorption of Gelbstoff at longer wavelengths for a given fraction of fulvic acid (Fig. 4).

The relative importance of light absorption by dissolved humus vs. by Gelbstoff in the ocean can perhaps be best appreciated by comparing $a_g(440)$ to $a_\phi(440)$, absorption by phytoplankton, the primary absorption variable in the ocean. One can express $a_\phi(440)$ as

$$a_\phi(440) = a^*_\phi(440)\ [\text{Chl } a] \qquad (2)$$

where $a^*_\phi(440)$ ($m^2\ mg^{-1}$) is the absorption per unit of chlorophyll a + pheophytin a, and [Chl a] is the concentration of chlorophyll a + pheophytin a (mg m^{-3}). Values for $a^*_\phi(440)$ can be determined for high concentrations of chlorophyll by the method of Morel and Bricaud (1981) or for lower concentrations by the methods of Mitchell and Kiefer (1984) or Carder et al. (1986*a*). However, $a^*_\phi(440)$ varies inversely as a function of phytoplankton cell size (Morel and Bri-

Table 3. Variation of the spectral slope for Gelbstoff as a function of the fulvic acid fraction for different spectral ranges for the Gulf of Mexico data.

Station	Depth (m)	Fulvic fraction	S_g (*f*, 370, 440)	S_g (*f*, 440, 565)
Mississippi	3	0.828	0.0128	0.0118
plume	3	0.909	0.0141	0.0127
	4	0.837	0.0129	0.0118
Gulf loop	20	0.966	0.0161	0.0146
intrusion	20	0.984	0.0172	0.0161
	20	0.944	0.0151	0.0136
	55	0.866	0.0133	0.0121
Yucatan	10	0.885	0.0136	0.0123
Campeche	5	0.878	0.0135	0.0122
Cape San	4	0.624	0.0115	0.0110
Blas	55	0.933	0.0148	0.0132

Note: Large fulvic fraction and S_g values in oligotrophic surface waters; small fulvic fraction and S_g values in products of senescent bloom degradation at shallow Cape San Blas station.

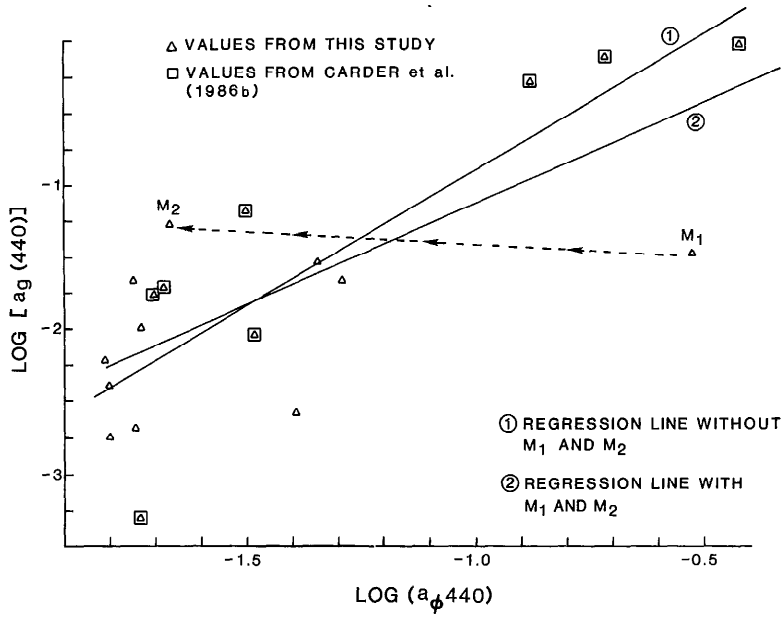

Fig. 5. Comparison between the absorption due to Gelbstoff and chlorophyll-like pigments for this study and for an earlier study. Note that point M_1 represents a fresh bloom in Mississippi plume waters which degraded over a 1.5-week period to point M_2.

caud 1981), and phytoplankton cell size empirically appears to vary as a function of [Chl *a*] (Carder et al. 1986*b*; Herbland et al. 1985). Thus, $a^*_\phi(440)$ can be expressed as a function of [Chl *a*] at least for the Gulf of Mexico (Carder et al. 1986*b*):

$$a^*_\phi(440) \doteq 0.0173 + 0.01435\,[\text{Chl } a]^{-1} \quad \text{for [Chl } a] \geq 0.7;$$
$$a^*_\phi(440) \doteq 0.0378 \text{ for [Chl } a] < 0.7; \quad (3)$$
$$a^*_\phi(565) \doteq 0.006. \quad (4)$$

Based on Figure 2 of Carder et al. (1986*b*), it also appears that a reasonable value for $a^*_\phi(550)$ would be about 0.0065 m^2 mg^{-1}. These equations include absorption effects due to phytoplankton as well as other particulates, since they were based upon the absorption of particles captured on filter pads.

Applying Eq. 2 and 3 to the chlorophyll data of Table 2 permits us to compare (Fig. 5) the relative absorption contributions of chlorophyll and Gelbstoff. Two things are apparent about the absorption due to MHA and MFA. First, these acids appear to account for most if not all of the absorption due to dissolved organic material in the GOM, because these calculated $a_g(440)$ values are consistent with those determined by Carder et al. (1986*b*) relative to the chlorophyll absorption present. Secondly, there is great variability in the data, suggesting that phytoplankton and marine humus are only weakly covariant. This lack of correspondence perhaps is due to significantly longer residence times for marine humus than for chlorophyll pigments and quite variable flushing and mixing rates for different regions.

An indication of the optical effects of a transition from a high chlorophyll bloom (7.9 mg m^{-3}) with moderate Gelbstoff [$a_g(440) = 0.0335$ m^{-1}) in the Mississippi plume ($S \doteq 25‰$) to its low chlorophyll (0.4 mg m^3), high Gelbstoff (0.0537 m^{-1}) residual found about 1.5 weeks later near Cape San Blas is demonstrated by the dashed line running from M1 to M2 on Fig. 5. The absorption coefficient due to phytoplankton and other particles, $a_\phi(440)$, was reduced by a factor of 13 during that transition, probably due mostly to grazing. On the other hand, the absorption coefficient due to

Table 4. Remote-sensing reflectance equations dependent on $a^*_g(\lambda)$ and [Chl *a*] (based on Carder et al. 1986*b*).

[Chl a] ≤ 0.70 mg m^{-3}

$$R_{RS}(440) = \frac{0.1076\{0.00242 + 0.0148\,(1.2)\,[\text{Chl a}]^{0.851}\}}{0.0145 + 0.037\,[\text{Chl a}] + a_g(440)} \quad (9)$$

$$R_{RS}(565) = \frac{0.1076\,(0.000872 + 0.0148\,[\text{Chl a}]^{0.851})}{0.07874 + 0.006\,[\text{Chl a}] + a_g(565)} \quad (10)$$

$$R_{RS}(550) = \frac{0.1076\,(0.00095 + 0.0148\,[\text{Chl a}]^{0.851})}{0.0638 + 0.0065\,[\text{Chl a}] + a_g(550)} \quad (11)$$

[Chl a] > 0.70 mg m^{-3}

$$R_{RS}(440) = \frac{0.1076\{0.00242 + 0.0148\,(1.2)\,[\text{Chl a}]^{0.851}\}}{0.0145 + 0.0173\,[\text{Chl a}] + 0.0143 + a_g(440)} \quad (12)$$

$$R_{RS}(565) = \frac{0.1076\,(0.000872 + 0.0148\,[\text{Chl a}]^{0.851})}{0.07874 + 0.006\,[\text{Chl a}] + a_g(565)} \quad (13)$$

$$R_{RS}(550) = \frac{0.1076\,(0.00095 + 0.0148\,[\text{Chl a}]^{0.851})}{0.0638 + 0.0065\,[\text{Chl a}] + a_g(550)} \quad (14)$$

Gelbstoff, $a_g(440)$, was increased by 60%, in spite of the dilution effect provided by mixing with offshore waters of high salinity and lower Gelbstoff.

For waters that do not go through the rapid transitions associated with phytoplankton population explosions followed by crashes in river plumes, upwelling areas, and spring blooms, a higher degree of coherence between $a_g(440)$ and $a_\phi(440)$ is expected. Under steady state conditions, the phase lag of $a_g(440)$ behind $a_\phi(440)$ and differences in residence times or degradation half-lives for the components are no longer important. It is interesting that the least-squares trendline bifurcates the dashed line from M1 to M2, suggesting that on average the least-squares trendline may be representative of steady state between the processes of phytoplankton growth and those of decay and mixing and flushing for a range of chlorophyll levels in the Gulf of Mexico. It is important to bear in mind that a reduction in flushing or mixing should allow degradation products to accumulate relative to a well-flushed environment. Thus a bay or stagnant gyre should have more Gelbstoff per unit of chlorophyll even without terrigenous inputs than would a recently upwelled phytoplankton bloom. As that bloom is transported offshore, however, and is grazed and degraded, it would likely follow a trend somewhat similar to the M1–M2 line in Fig. 5, resulting in high absorption of Gelbstoff per unit of chlorophyll. This transition should have significant ramifications on the algorithms for the remote measurement of chlorophyll pigments from space, especially offshore of highly productive upwelling regions and under early vs. late spring bloom conditions.

The most commonly applied chlorophyll algorithm used with CZCS data corrected for atmospheric effects is

$$[\text{Chl } a] = A(r_{ij})^B \quad (5)$$

where A and B are constants, and the spectral radiance ratio is

$$r_{ij} = L_u(\lambda_i)[L_u(\lambda_j)]^{-1}. \quad (6)$$

$L_u(\lambda)$ is the subsurface upwelling radiance at wavelength λ, and i and j represent two different wavelengths (e.g. 443 and 550 nm) (Gordon and Morel 1983).

Equation 6 can also be expressed as

$$r_{ij} = R_{RS}(\lambda_i)[R_{RS}(\lambda_j)]^{-1} \quad (7)$$

since

$$R_{RS}(\lambda) = \pi L_w(\lambda)[E_T(\lambda)]^{-1} = IL_u(\lambda)[E_T(\lambda)]^{-1}.$$

Here $R_R(\lambda)$ is the remote sensing reflectance, $E_T(\lambda)$ is the total (sunlight + skylight) downwelling irradiance, $L_w(\lambda)$ is the water-leaving upwelling radiance, and I is a spectrally constant function representing the radiance distribution effects and the transmissivity and radiance divergence across the sea–air interface (*see* Austin 1974).

Based on the work of Morel and Prieur (1977) and Bricaud et al. (1983), Carder and Steward (1985) have shown that

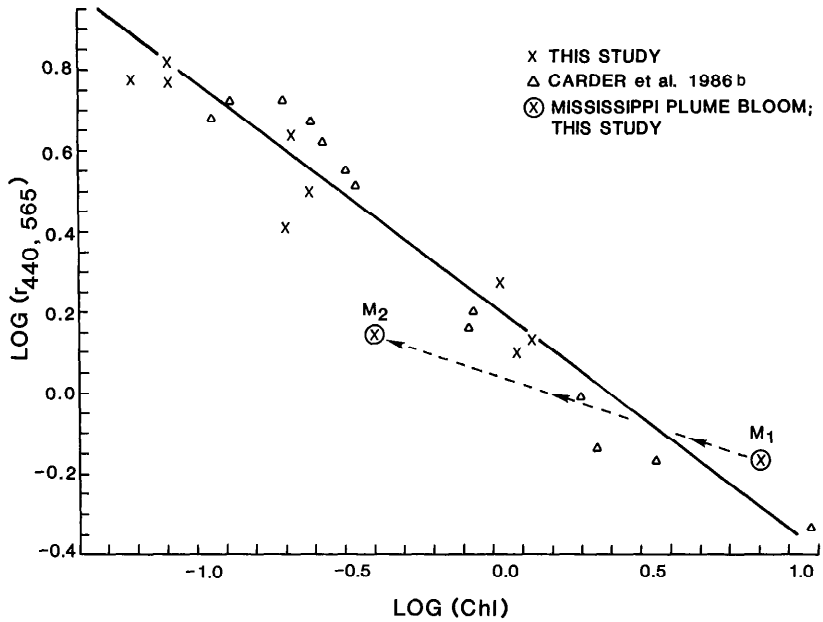

Fig. 6. Comparison of modeled reflectance ratio data vs. chlorophyll data from this study to measured data from Carder et al. (1986*b*) for the Gulf of Mexico. Also shown are the 1.5-week "bloom degradation" transition line between M_1 and M_2 and the least-squares regression line for the "case 1" data points of this study and Carder et al. (1986*b*) combined; i.e. points M_1 and M_2 were excluded from the regression with the case 1 exclusivity test of Gordon and Morel (1983).

$$R_{RS} = 0.1076(b'_w + b'_p) \times (a_w + a_g + a^*_p[\text{Chl } a])^{-1} \quad (8)$$

here the b' represents backscattering and the subscripts represent water, particulate, and Gelbstoff contributions to backscattering and absorption. The wavelength dependence of the variables is not shown for convenience. The particle chlorophyll-specific absorption coefficient a^*_p is usually dominated by a^*_ϕ, the phytoplankton chlorophyll-specific absorption coefficient. Tables are available for the water backscattering (Morel 1974) and absorption coefficients (Smith and Baker 1981), and Carder et al. (1986*b*) have developed empirical relationships for b'_p and a^*_p for the Gulf of Mexico as a function of [Chl *a*]. Their a^*_p relationship accounts for the cell size or package effects on phytoplankton and other particulate absorption (e.g. by detritus) for GOM samples. If we assume that the cell size or package effect is fairly universal (*see* Morel and Bricaud 1981), the application of these relationships to other waters may be correct to first order.

Combining Eq. 3, 4, 7, and 8 for $\lambda_i = 440$ nm and $\lambda_j = 565$ nm or $\lambda_j = 550$ nm, we arrive at (Carder et al. 1986*b*) Eq. 9–14 in Table 4. We have assumed that the spectral ratio of particle backscatter, $b'_p(440)$: $b'_p(565)$, has a value of 1.2 in Table 4. It typically ranges between 1.0 and 1.4 for the Gulf of Mexico (Carder et al. 1986*b*). The effects of the measured values of $a_g(\lambda)$ and [Chl *a*] listed in Table 2 on the remote-sensing reflectance ratio $r_{440,565}$ can be modeled using the equations in Table 4. Here $r_{440,565} = R_{RS}(440)/R_{RS}(565)$. Figure 6 compares the modeled GOM data for 1980 and 1981 from this study to the measured GOM data for 1984 of Carder et al. (1986*b*) and also shows the least-squares regression line (solid) for the data and the trendline (M1–M2) associated with the senescence and degradation of a bloom over a 1.5-week period. The slope of the relation ($B = -1.83$) is quite close to the value of -1.80 reported

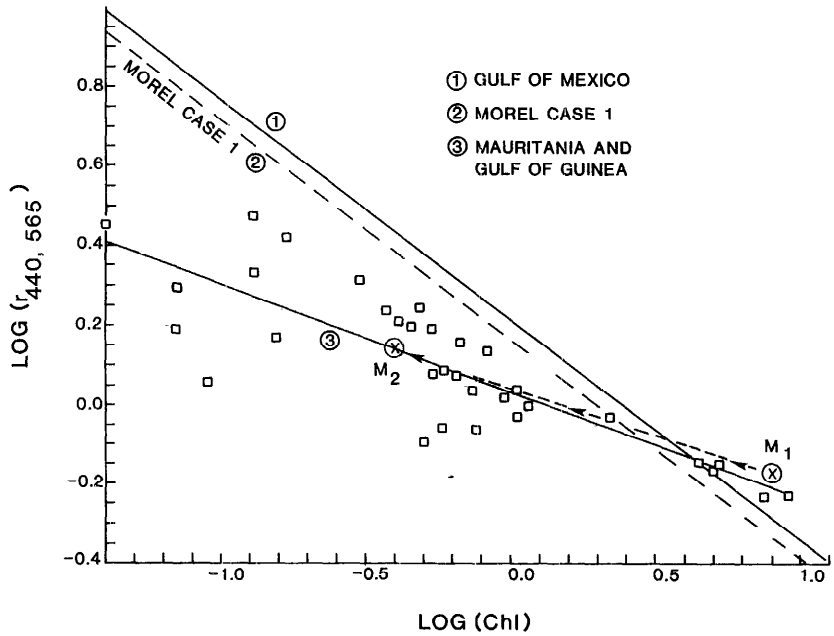

Fig. 7. Modeled reflectance ratio vs. chlorophyll data with the data of Bricaud et al. (1981) for Gelbstoff and chlorophyll for the Gulf of Guinea and Mauritanian waters. Also shown are the Gulf of Mexico regression line and M_1 and M_2 trendlines from Fig. 6, and the regression line for the case 1 water data of Morel (1980).

by Gordon and Morel (1983) for case 1 waters. Removal of points M1 and M2 in the regression provides a better representation of steady-state conditions for case 1 waters in the Gulf of Mexico, with a correlation coefficient of 0.976.

The similarity between modeled and field remote-sensing reflectance data for different years, locations, and multiple seasons suggests three things: the cell size or package effect on $a^*_p(\lambda)$ incorporated in the model apparently is independent of season and thus probably species, $b'_p(\lambda)$ for these waters apparently covaries reasonably well with [Chl *a*] as specified by the model, and marine humic and fulvic acids apparently account for most if not all of the absorption due to dissolved materials in the Gulf of Mexico.

The trendline between M1 and M2 may also be indicative of the directionality that a regression line would take on a similar plot for an upwelling region. To test this hypothesis, the chlorophyll pigment and Gelbstoff data of Bricaud et al. (1981) from the coastal upwelling area off Mauritania and from the equatorial divergence region in the Gulf of Guinea were used in the model of remote-sensing reflectance (Fig. 7). Doing so provides a first-order estimate of the $r_{440,\,565}$ values associated with various pigment levels for an upwelling region with high levels of residual Gelbstoff. Note the similarity in slope between the M1–M2 line and the regression line ($B = -3.73$) in Fig. 7, suggesting that the waters low in chlorophyll adjacent to a highly productive region have excessive Gelbstoff relative to case 1 waters.

For the productive waters of the Southern California Bight region, Smith and Baker (1982) found a B value of -2.59. Although this slope is not as steep as was found off northwest Africa, the primary productivity of the African study region may have been higher than that off southern California. The "squirts" and "jets" off southern California also suggest a higher degree of flushing of degradation products for this region than perhaps occurs in the Gulf of Guinea.

Gelbstoff can be considered as a by-product of primary productivity by plotting literature values of $a_g(440)$ (Fig. 8) against lit-

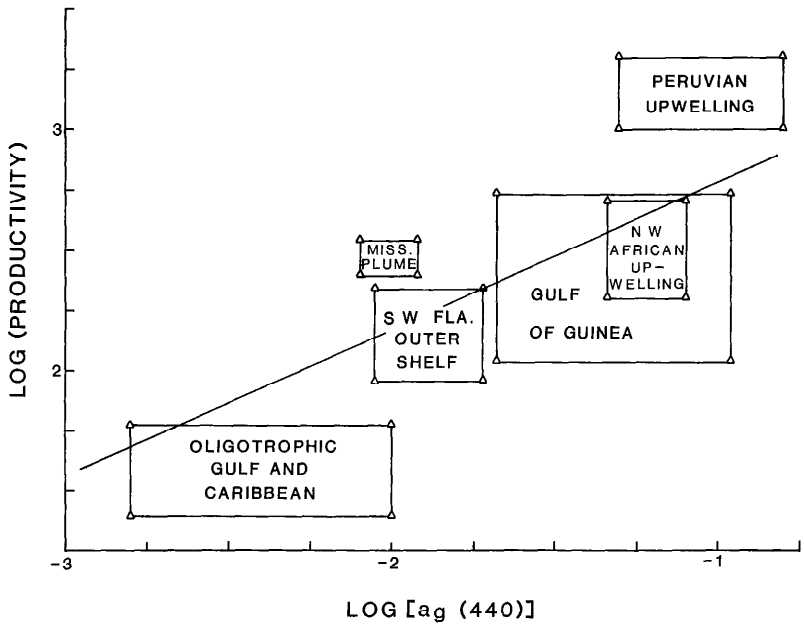

Fig. 8. Relationship between annual primary productivity and marine Gelbstoff absorption based on literature values. The rectangles enclose ranges of Gelbstoff and primary productivity reported for the oligotrophic Gulf of Mexico and Caribbean, Mississippi plume, outer Florida Shelf, NW African upwelling (Mauritanian coastal waters), Gulf of Guinea, and the Peruvian upwelling. Data sources are listed in Table 5.

erature values (Table 5) of primary productivity (g C m^{-2} yr^{-1}). If the numbers reported were truly areal and annual averages for both variables, and if terrigenous inputs are negligible for these various regions, then the flushing or mixing rate of the degradation products of primary production might be considered the major variable affecting the scatter amongst these points. Even so it is clear that a general relationship exists between Gelbstoff and primary productivity which may ultimately be refined to the point that residual Gelbstoff pools may be interpretable as a measure of the primary productivity of a region over the previous 1 or 2 months. For this approach to be useful, a better understanding of degradation rates from chlorophyll to MFA to MHA is required as well as the effects of flushing, mixing, and photolysis on the degradation product. Even without these more intense studies, a certain degree

Table 5. Data sources for comparisons of $a_g(440)$ with primary productivity for various near-surface waters.

Location	Data sources for ranges of	
	primary productivity	$a_g(440)$
Oligotrophic Gulf of Mexico and Caribbean	El Sayed 1972; Steven 1971	This study
Outer SW Florida shelf	Yoder et al. 1987	Hojerslev 1985*; Carder et al. 1986*b*
Mississippi plume	Thomas and Simmons 1960; Fucik 1974	This study
NW African upwelling	Huntsman and Barber 1977	Bricaud et al. 1981
Gulf of Guinea	Voituriez and Herbland† 1979	Bricaud et al. 1981
Peruvian upwelling	Walsh 1983	Burt 1958

* Extrapolated from 371 nm; based on E_d(10 m) measurements − K_w(370) values for water (Smith and Baker 1981).
† Assumed annualized 9 h × 365 d of effective sunlight; range from warm- and cold-water seasons.

of accuracy can be expected from empirical studies of primary productivity vs. Gelbstoff. The promise of wavelengths near 400 nm on future ocean color sensors on satellites to help in measuring Gelbstoff bodes well for improvements in the accuracy of ocean chlorophyll measurements from space and perhaps for a more direct way to infer from space the history of primary productivity for a parcel of water or a region.

References

AUSTIN, R. W. 1974. Inherent spectral radiance signatures of the ocean surface, p. 2.1–2.20. *In* Ocean color analysis. Scripps Inst. Oceanogr. Ref. 74-10.

BRICAUD, A., A. MOREL, AND L. PRIEUR. 1981. Absorption by dissolved organic matter in the sea (yellow substance) in the UV and visible domains. Limnol. Oceanogr. **26:** 43–53.

———, ———, AND ———. 1983. Optical efficiency factors of some phytoplankters. Limnol. Oceanogr. **28:** 816–832.

BURT, W. V. 1958. Selective transmission of light in tropical Pacific waters. Deep-Sea Res. **5:** 51–61.

CARDER, K. L., AND OTHERS. 1986*a*. The interaction of light with phytoplankton in the marine environment, p. 42–55. *In* Ocean optics 8. Proc. Soc. Photo-Opt. Instr. Eng. 637.

———, AND R. G. STEWARD. 1985. A remote-sensing reflectance model of a red-tide dinoflagellate off west Florida. Limnol. Oceanogr. **30:** 286–298.

———, ———, J. H. PAUL, AND G. A. VARGO. 1986*b*. Relationships between chlorophyll and ocean color constituents as they affect remote-sensing reflectance models. Limnol. Oceanogr. **31:** 403–413.

EL SAYED, S. Z. 1972. Primary productivity and standing crop of phytoplankton, p. 8–13. *In* Chemistry, primary production, and benthic algae of the Gulf of Mexico. Ser. Atlas Mar. Environ., Am. Geogr. Soc. 22.

FOGG, F. E., AND G. T. BOALCH. 1958. Extracellular products in pure cultures of brown alga. Nature **181:** 789–790.

FUCIK, K. W. 1974. The effect of petroleum operations on the phytoplankton ecology of the Louisiana coastal waters. M.S. thesis, Texas A&M Univ. 82 p.

GORDON, H. R., AND A. Y. MOREL. 1983. Remote assessment of ocean color for interpretation of satellite visible imagery: A review. Springer.

HARVEY, G. R., D. A. BORAN, L. A. CHESAL, AND J. M. TOKAR. 1983. The structure of marine fulvic and humic acids. Mar. Chem. **12:** 119–132.

HAYASE, K., AND H. TSUBOTA. 1985. Sedimentary humic acid and fulvic acid as fluorescent organic materials. Geochim. Cosmochim. Acta **49:** 159–163.

HERBLAND, A., A. LE BOUTEILLER, AND R. RAIMBAULT. 1985. Size structure of phytoplankton biomass in the equatorial Atlantic Ocean. Deep-Sea Res. **32:** 819–836.

HOJERSLEV, N. K. 1974. Inherent and apparent optical properties of the Baltic. Univ. Copenhagen Inst. Phys. Oceanogr. Rep. 23. 70 p.

———. 1985. Bio-optical measurements in the southwest Florida shelf ecosystem. J. Cons. Cons. Int. Explor. Mer **42:** 65–82.

HUNTSMAN, S. A., AND R. T. BARBER. 1977. Primary production off northwest Africa: The relationship to wind and nutrient conditions. Deep-Sea Res. **24:** 25–33.

JAMES, H. R., AND E. A. BIRGE. 1938. A laboratory study of the absorption of light by lake waters. Trans. Wis. Acad. Sci. **31:** 1–154.

JERLOV, N. G. 1955. Factors influencing the transparency of the Baltic waters. Medd. Oceanogr. Inst. Goteborg 25. 19 p.

———. 1968. Optical oceanography. Elsevier.

KALLE, K. 1966. The problem of Gelbstoff in the sea. Oceanogr. Mar. Biol. Annu. Rev. **4:** 91–104.

KIRK, J. T. O. 1980. Spectral absorption properties of natural waters: Contribution of the soluble and particulate fractions to light absorption in some inland waters of southeastern Australia. Aust. J. Mar. Freshwater Res. **31:** 287–296.

LUNDGREN, B. 1976. Spectral transmittance measurements in the Baltic. Univ. Copenhagen Inst. Phys. Oceanogr. Rep. 30. 38 p.

MITCHELL, B. G., AND D. A. KIEFER. 1984. Determination of absorption and fluorescence excitation spectra for phytoplankton, p. 157–169. *In* O. Holm-Hansen et al. [eds.], Marine phytoplankton and productivity. Springer.

MOREL, A. Y. 1974. Optical properties of pure water and sea water, p. 1–24. *In* N. G. Jerlov and E. Steemann Nielsen [eds.], Optical aspects of oceanography. Academic.

———. 1980. In-water and remote measurement of ocean color. Boundary-Layer Meteorol. **18:** 177–201.

———, AND A. BRICAUD. 1981. Theoretical results concerning light absorption in a discrete medium and application to the specific absorption of phytoplankton. Deep-Sea Res. **28:** 1357–1393.

———, AND L. PRIEUR. 1975. Analyse spectrale de l'absorption par les substances dissoutes (substances jaunes), p. 1–9. *In* Résultats de la campagne CINECA 5 (Groupe Médiprod), Sect. 1-1-11. Publ. CNEXO.

———, AND ———. 1977. Analysis of variations in ocean color. Limnol. Oceanogr. **22:** 709–722.

SMITH, R. C., AND K. A. BAKER. 1981. Optical properties of the clearest natural waters (200–800 nm). Appl. Opt. **20:** 177–184.

———, AND ———. 1982. Oceanic chlorophyll concentrations as determiend by satellite (Nimbus-7 Coastal Zone Color Scanner). Mar. Biol. **66:** 269–279.

STEVEN, D. M. 1971. Primary productivity of the tropical western Atlantic Ocean near Barbados. Mar. Biol. **10:** 261–264.

STUERMER, R. H. 1975. The characterization of humic substances in sea water. Ph.D. thesis, Mass. Inst. Technol., Woods Hole Oceanogr. Inst. 163 p.

THOMAS, W. J., AND E. G. SIMMONS. 1960. Phyto-

plankton production in the Mississippi Delta, p. 103–116. *In* F. P. Shepard et al. [eds.], Recent sediments, northwest Gulf of Mexico. Publ. Am. Assoc. Pet. Geol.

VOITURIEZ, B., AND A. HERBLAND. 1979. The use of the salinity maximum of the Equatorial Undercurrent for estimating nutrient enrichment and primary productivity in the Gulf of Guinea. Deep-Sea Res. **26:** 77–83.

WALSH, J. J. 1983. Death in the sea: Enigmatic phytoplankton losses. Prog. Oceanogr. **12:** 1–86.

YENTSCH, C. S., AND C. A. REICHERT. 1962. The interrelationship between water-soluble yellow substances and chloroplastic pigments in marine algae. Bot. Mar. **3:** 65–74.

YODER, J. A., C. R. MCLAIN, J. O. BLANTON, AND L.-Y. OEY. 1987. Spatial scales in CZCS-chlorophyll imagery of the southeastern U.S. continental shelf. Limnol. Oceanogr. **32:** 929–941.

ZEPP, R. G., AND P. F. SCHLOTZHAUER. 1981. Comparison of photochemical behavior of various humic substances in water: 3. Spectroscopic properties of humic substances. Chemosphere **10:** 479–486.

Submitted: 30 September 1987
Accepted: 9 June 1988
Revised: 10 October 1988